^{102}Pd: An E(5) nucleus?

N. V. Zamfir,[1,2,3] M. A. Caprio,[1] R. F. Casten,[1] C. J. Barton,[1] C. W. Beausang,[1] Z. Berant,[1,2,4] D. S. Brenner,[2] W. T. Chou,[1,5] J. R. Cooper,[1] A. A. Hecht,[1] R. Krücken,[1] H. Newman,[1,6] J. R. Novak,[1] N. Pietralla,[1] A. Wolf,[1,2,4] and K. E. Zyromski[1]

[1] *Wright Nuclear Structure Laboratory, Yale University, New Haven, Connecticut 06520*

[2] *Clark University, Worcester, Massachusetts 01610*

[3] *National Institute for Physics and Nuclear Engineering, Bucharest-Magurele, Romania*

[4] *Nuclear Research Center Negev, Beer-Sheva, Israel*

[5] *National Tsing Hua University, Hsinchu, Taiwan, Republic of China*

[6] *University of Surrey, Guildford, Surrey GU2 7XH, United Kingdom*

(Received 28 November 2001; published 3 April 2002)

In this paper states in ^{102}Pd populated in the ϵ/β^+ decay of ^{102}Ag, produced in the ^{89}Y(^{16}O,3n) reaction, were studied with high efficiency Ge detectors. The level scheme of ^{102}Pd is in good overall agreement with the predictions of the E(5) critical point symmetry, with the exception of the 0_2^+ state, which may be of intruder character.

DOI: 10.1103/PhysRevC.65.044325 PACS number(s): 21.10.−k, 21.60.Ev, 23.20.Lv, 27.60.+j

I. INTRODUCTION

Nuclear collectivity is often described in the context of a harmonic vibrator [1], a deformed symmetric rotor [2], and γ-unstable [3] models, which constitute a set of idealized limits. These three limits have been codified in the framework of the interacting boson approximation (IBA) model [4] in terms of the U(5), SU(3), and O(6) dynamical symmetries, respectively. Figure 1 shows Casten's triangle for the IBA where each vertex represents one of the three symmetries mentioned above, and the legs denote regions in which the structure undergoes a transition from one limit to another. There are few nuclei close to the dynamical symmetry limits, but the vast majority are transitional and must, therefore, be described by numerical diagonalizations of a multiparameter Hamiltonian. It was shown in Ref. [5], using the intrinsic state formalism of the IBA, that there are phase/shape transitions in the evolution of nuclear shapes from spherical to deformed. Of course, phase transitional behavior in finite nuclei will be muted compared to infinite systems. Nevertheless, recently, Iachello introduced new dynamical symmetries at the critical point of such phase transitions: E(5) for a transition between spherical and deformed γ-soft nuclei [6] and X(5) for a transition between spherical and axially deformed nuclei [7]. His approach was based on analytic solutions of the differential equation for a geometric (Bohr) Hamiltonian with a flat-bottomed potential in the quadrupole deformation. The E(5) symmetry can be used to describe nuclei that are at the critical point of the U(5)-O(6) transition and ^{134}Ba has been found to be close to this symmetry [8]. The X(5) symmetry is exemplified by ^{152}Sm [9], ^{150}Nd [10], and possibly other $N=90$ isotones.

The Pd isotopes are another typical example of U(5)-O(6) transitional nuclei. In fact, they were successfully reproduced in terms of a transition from U(5) to O(6) in the framework of IBA-1 [11,12] or IBA-2 [13–15]. They were also calculated by Pan and Draayer [16] with a parametrized exact solution for the U(5)-O(6) transition within the SU(1,1) algebra. The positive parity excitation spectra of light Pd isotopes were also successfully reproduced by adding quartic anharmonicities to an O(5) Hamiltonian [17]. All these results suggest that ^{102}Pd is located in the middle of the transition from U(5) to O(6), potentially very close to the critical point of the shape/phase transition, and is, therefore, a very good candidate for the recently introduced E(5) symmetry.

The goal of this work is to measure with high accuracy the intensities of the transitions depopulating the members of potential multiphonon states in ^{102}Pd and to compare their level scheme with the E(5) predictions.

II. EXPERIMENT

The low-lying nonyrast states of ^{102}Pd were populated in the ϵ/β^+ decay of the 5^+ ($T_{1/2}=12.9$ min) ground state of ^{102}Ag and studied through γ-ray spectroscopy at the Yale Moving Tape Collector [18]. The parent nuclei were produced through the ^{89}Y(^{16}O,3n) reaction. A 5-mg/cm^2 target on a 2-mg/cm^2 Au backing, facing the beam, was bombarded with a 20 pnA, 75-MeV ^{16}O beam provided by the ESTU Tandem at WNSL at Yale University. The recoil products were collected on a 16-mm-wide aluminized

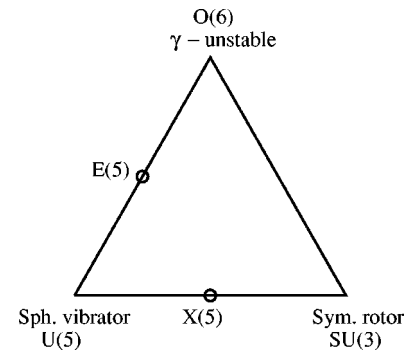

FIG. 1. Casten's symmetry triangle with the new critical point solutions E(5) and X(5) [6,7]. The labels at the vertices are those of the dynamical symmetries of the IBA, denoting subchain decompositions of U(6), while E(5) and X(5) label solutions to particular geometric potentials in a differential operator Hamiltonian.

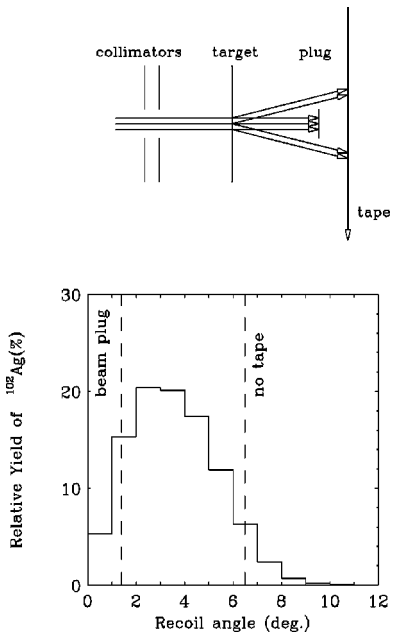

FIG. 2. Top: Schematic design of the plug technique at the Yale Moving Tape Collector. Bottom: Angular distribution of the ^{102}Ag product in the present experiment according to statistical model (code PACE) [19] calculations. Those residual nuclei from the ^{89}Y(^{16}O,3n) reaction, scattered at angles between $\sim$1.5° and $\sim$6.5°, are collected on the tape for transport to the counting area.

Kapton tape and transported to a low background counting area.

In order to stop the primary beam and to prevent burning the tape, a plug technique [18], sketched in Fig. 2 (top), was used. The target was located behind a set of two collimators that define a 3-mm-diameter beam spot. The unreacted primary beam particles were stopped on the 3-mm-diameter plug, positioned $\sim$6 cm behind the target and in front of the tape. In contrast, most fusion evaporation products bypass the plug and were collected on the Kapton tape positioned $\sim$7 cm behind the target. In this geometry the collecting angles for the reaction products were between $\sim$1.5° and $\sim$6.5°, corresponding to the maximum yield for the residual nuclei. This simple geometric arrangement suppressed more than 99% of the primary beam while $\sim$80% of the residual nuclei were deposited on the tape (see Fig. 2, bottom) and transported in front of the detectors. The sequencing of the tape movements was 20 min in order to enhance the yield for ^{102}Pd (given the 12.9 min half-life for the ground state of ^{102}Ag).

The γ rays were detected with an array consisting of three Compton-suppressed segmented Clover HPGe detectors and one LEPS detector in close geometry, with a total photopeak efficiency of $\sim$2% at 1.33 MeV. γ-ray singles and γ-γ coincidence data were simultaneously acquired in event mode. A singles spectrum is shown in Fig. 3(a) and a γ-γ spectrum, gated on the 556-keV $2_1^+ \rightarrow 0_1^+$ transition, is shown in Fig. 3(b). The energy range of the spectrum was limited to $E_\gamma^{max} \sim 2.3$ MeV.

Table I lists the γ rays observed in this work and, based on γ-γ coincidences, placed in the level scheme of ^{102}Pd.

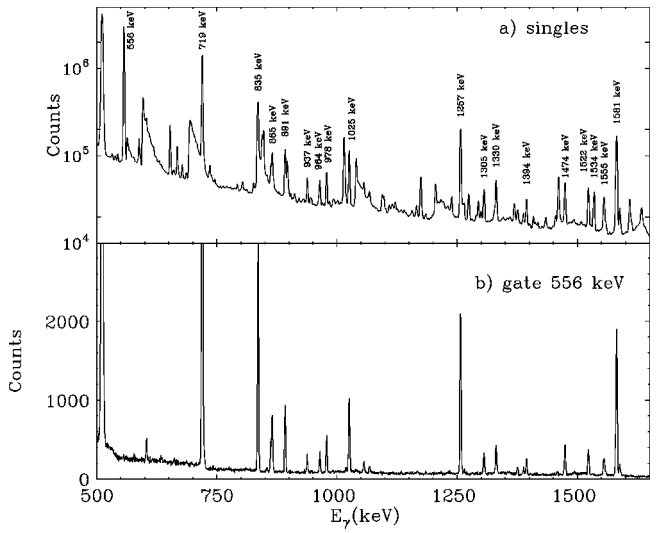

FIG. 3. Examples of γ-ray data from the present measurements. The most intense γ transitions assigned to ^{102}Pd are marked in the singles spectrum.

Figure 4 shows the level scheme as deduced in this work.

As specified in Table I, there are a few γ transitions that are reported for the first time. Here we discuss only those that are important for the lowest quadrupole multiphonon structure of this nucleus.

(1) The 3_1^+ state at 2112 keV was reported previously to decay only through the 1555-keV transition to the 2_1^+ state [20]. Two additional transitions of 577 and 836 keV were observed to populate the 2_2^+ and 4_1^+ states, respectively. The experimental relative $B(E2)$ values (with the assumption that the transitions have a pure $E2$ character) for the transitions from this state to the 4_1^+, 2_2^+, and 2_1^+ states are in the ratio 1:7(4):0.4(2). This decay pattern is consistent with the interpretation of this state as a three-phonon vibrational state.

(2) The transition of 964 keV deexciting the state at 3075 keV with spins 4^+,5^+,6^+ was found to be a doublet: γ-γ coincidence data revealed that there are, in fact, two transitions of 963.3 keV and 964.2 keV to the 3_1^+ and 6_1^+ states, respectively. Based on the new transition to the 3_1^+ state, the spin value of the 3075-keV level is now restricted to 4^+ or 5^+, because an $M3;6^+ \rightarrow 3^+$ transition is extremely unlikely. This state is a very good candidate for the 4^+ member of the four-phonon multiplet.

There are two known excited 0^+ states at 1592 keV and 1658 keV [21–24], which, however, are not observed in the present experiment. They were seen in the ϵ/β^+ decay from the 2^+ ($T_{1/2}=7.7$ min) state in ^{102}Ag [21], a state that was not populated in our experiment. The 1592-keV state has been shown to decay by an $E0$ transition to the ground state with $\rho^2=4.0(15)\times10^{-3}$ and by an $E2$ transition of 96 (40) W.u. to the 2_2^+ state [23]. An upper limit of $<4\times10^{-4}$ W.u. was established for the $B(E2:0_2^+ \rightarrow 2_1^+)$ value [23]. The 1658-keV state decays via an $E2$ transition of 13 (3) W.u. to the 2_1^+ state and with an upper limit of $\rho^2<0.3\times10^{-3}$ for the monopole strength of the $E0(0_3^+ \rightarrow 0_1^+)$ transition [23]. We include the 0^+ states in the discussion presented in the following section.

TABLE I. γ rays assigned to ^{102}Pd. (Intensities are obtained from singles data or γ-γ coincidences and are normalized to 10 000 for the 556-keV $2_1^+ \rightarrow 0_1^+$ transition.)

E_γ (keV)	$I_{\rm rel}$	E_{x_i}-E_{x_f}
163.0(1) [a]	25(5) [b]	2301-2138
179.8(2) [c]	9(2)	2474 [d]-2294
182.5(1) [c]	15(3) [b]	2294 [d]-2112
231.7(1) [a]	21(2)	2532-2301
336.4(2) [c]	18(2)	2474 [d]-2138
424.4(1) [a]	7(2)	3075-2651
495.0(1) [a]	59(6)	2606 [d]-2112
539.6(4)	6(3) [b]	2651-2111
556.44(4)	10000	556-0
577.1(1) [a]	17(3) [b]	2112 -1534
603.32(6)	161(14)	2138-1534
634.1(1) [a]	19(3)	3166 -2532
660.5(1) [a]	20(10)	2798-2138
719.33(5)	5590(150)	1276-556
835.11(7)	1261(105) [b]	2111-1276
836.0(5) [a]	15(8) [b]	2112-1276
854.3(1) [a]	17(10)	2798-1944
861.9(1)	159(14) [e]	2138-1276
865.0(2)	270(25)	2976-2111
891.6(1)	384(35)	3003-2111
937.7(2)	139(12)	3075-2138
946.4(1) [a]	18(2)	2481 [d]-1534
963.3(5) [e]	21(10) [b]	3075- 2112
964.2(1) [e]	122(11) [b]	3075-2111
977.75(5)	181(16)	1534-556
998.3(3) [a]	9(3) [b]	2532-1534
1018.5(5) [c]	25(5)	2294 [d]- 1276
1024.9(1)	438(44)	2301-1276
1054.9(5) [a]	11(5) [b]	3166-2112
1055.4(2)	59(7) [b]	3166-2111
1066 [f]	18(8) [b]	2342 -1276
1067.2(1)	41(6) [b]	3178 [g]-2111
1167.5(8) [a]	3(1)	3278 [g]-2111
1184.5(5) [a]	21(2)	3295 [g]-2111
1215.5(3) [a]	11(3)	2750 [g]- 1534
1256.7(1)	1170(70)	2532-1276
1263.9(1) [a]	69(7)	2798-1534
1305.4(1)	166(17)	2581 [g]-1276
1329.1(1) [a]	33(7) [b]	2863 [g] - 1534
1330.5(1) [c]	190(28) [b]	2606 [d]-1276
1375.2(1)	53(6)	2651 [d]-1276
1387.4(2)	21(14)	1944-556
1393.7(2)	114(12)	2669 [g] -1276
1458.1(2) [c]	16(2)	2734 [d]- 1276
1474.0(1) [h]	238(25)	2750 [g]-1276
1492.6(1) [c]	14(2)	2768 [d]-1276
1522.5(1)	203(21)	2798 -1276
1534.3(1)	193(21)	1534-0
1555.1(1)	144(15)	2112-556
1581.1(1)	1292(80)	2138-556
1587.7(2) [a]	101(11)	2863 [g] - 1276
1691.3(3)	15(2)	2248-556
1700.4(3) [a]	13(2)	2976-1276
1727.9(3) [a]	25(3)	3003-1276
1744.3(1)	1426(75)	2301-556
1785.8(2) [c]	14(3)	2342 [d]- 556
1799.5(1)	223(24)	3075-1276
1837.3(3) [a]	78(9)	3113 [g]- 1276
1889.4(3)	40(5)	3166-1276
1924.1(2) [c]	54(6)	2481 [d]- 556
1943.0(9)	18(10)	1944-0
1976.0(3) [a]	9(5)	2532-556
2241.6(8)	60(10)	2798-556

[a]New γ transition relative to those reported in Ref. [20].
[b]γ-transition energy and intensity are obtained from coincidence spectra.
[c]New γ-ray transition in β decay (relative to those reported in Ref. [20]).
[d]New level in β decay.
[e]New intensity significantly different from previous data [20].
[f]Possible γ transition between the levels at 2342 keV (3_1^-) and 1276 keV (4_1^+). Since the γ-γ coincidence relations cannot distinguish this transition from that between the 3178- and 2111-keV levels, its placement is based on physics arguments and on different intensities in singles and coincidence spectra. It is not included in Fig. 4.
[g]New level relative to those reported in Ref. [20].
[h]New position relative to that reported in Ref. [20].

III. DISCUSSION

As mentioned in the Introduction, the Pd isotopes are typical examples of U(5)-O(6) transitional nuclei. With neutron number increasing from $N=50$, the quadrupole deformation also increases from small values, characteristic of a spherical vibrator ($N=52,54$), towards larger values, characteristic of deformed nuclei, in the middle of the shell. Figure 5 presents some of the experimental signatures of the structural evolution in this transition from a spherical vibrator to deformed γ-soft nuclei: the energy of the 2_1^+ state is decreasing and the ratio $R_{4/2} \equiv E(4_1^+)/E(2_1^+)$ is increasing with increasing number of valence neutrons. ^{102}Pd$_{56}$, which lies in the middle of this transitional region, is a very good candidate for the recently introduced E(5) symmetry, which applies to the critical point of the second-order phase transition between a spherical vibrator and a deformed γ-unstable nucleus.

The E(5) symmetry describes nuclei that are at the critical point of the U(5)-O(6) transition. An important signature is the ratio $R_{4/2} \equiv E(4_1^+)/E(2_1^+)$, which is intermediate ($R_{4/2}=2.20$) between a spherical vibrator or U(5) ($R_{4/2}=2.00$) and a deformed γ-unstable limit or O(6) ($R_{4/2}=2.50$). However, other essential signatures for an E(5) symmetry are the properties of the 0_2^+ and 0_3^+ states, which also vary along the U(5)-O(6) transition. Figure 6 shows typical low-lying spectra corresponding to the U(5) and O(6) limits. The multiplet

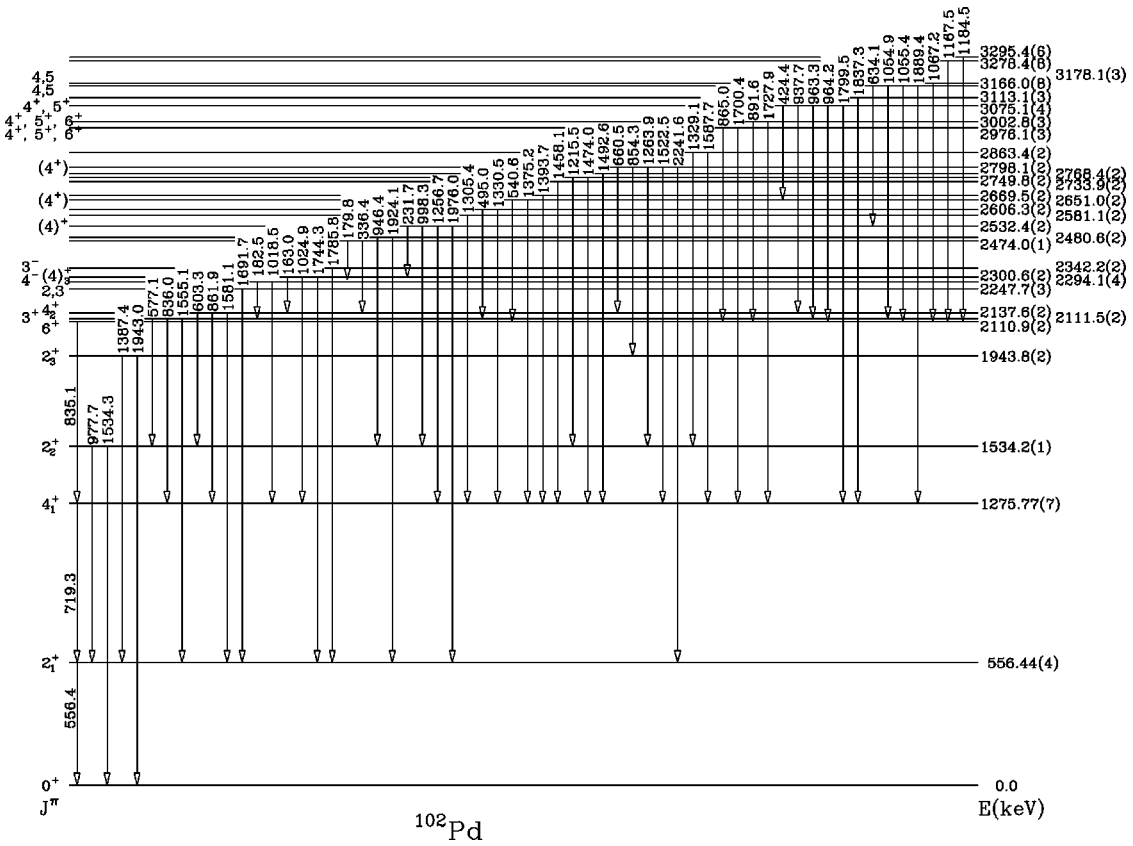

FIG. 4. Level scheme of ^{102}Pd as deduced in this work. The spin assignments are from Ref. [20] except the state at 3075 keV (see text).

structure is present in both limits, and all along the transition leg between them, since O(5) symmetry is preserved. A major difference between these two limits, besides the relative energies of the multiplets, is the structure of the excited 0^+ states. One is a member of the three-phonon multiplet in the entire transition from U(5) to O(6). The other one evolves from a two-phonon state in U(5), with a strong $B(E2{:}0^+ \rightarrow 2_1^+)$ value, into the $\sigma=\sigma_{\max}-2$, 0^+ state in O(6), where it typically lies higher than the 4_1^+ and 2_2^+ levels and the $B(E2)$ strength to the 2_1^+ level vanishes. In the discussion below we use the $E(5)$ notation 0_ξ^+ for this state and 0_τ^+ for the 0^+ member of the three-phonon multiplet.

In order to investigate the structure of ^{102}Pd we can exploit the IBA model. In this model a specific choice of parameters generates E(5) (for finite particle number) but variations of the parameters provide an easy way to explore the entire U(5)-O(6) path. An IBA Hamiltonian describing the transition between U(5) and O(6) is

$$H=\epsilon\hat{n}_d+a_0\hat{P}^\dagger\cdot\hat{P}+a_3\hat{T}_3\cdot\hat{T}_3, \tag{1}$$

where ϵ is the d-boson energy, $\hat{n}_d=d^\dagger\cdot\tilde{d}$ is the d-boson number operator, $\hat{P}=1/2[s\cdot s-\tilde{d}\cdot\tilde{d}]$, and $\hat{T}_3=(d^\dagger\tilde{d})^{(3)}$. This Hamiltonian displays the O(5) symmetry and the corresponding quantum number τ is a good quantum number. In the transition U(5)-O(6) there is a second-order phase transition. The critical point corresponds to a specific value of the control parameter $\eta\equiv 0.25a_0(N_B-1)/(\epsilon+7a_3/3)$, namely, $\eta_{crit}=0.25$ (N_B is the number of bosons, in this case five). $E2$ transitions are described in the IBA by the operator

$$T(E2)=e_2[s^\dagger\tilde{d}+d^\dagger s+\chi(d^\dagger\tilde{d})^{(2)}], \tag{2}$$

where e_2 is the boson effective charge. The transition strengths are calculated with $\chi=-\sqrt{7}/2$ and are normalized to the experimental value $B(E2{:}2_1^+\rightarrow 0_1^+)=33$ W.u., which corresponds to an effective charge $e_2=0.11eb$ in the quadrupole operator. The first term of the transition operator in Eq. (2) produces strict selection rules: only $\Delta\tau=\pm 1$ transitions are allowed. The second term does not modify these ''allowed'' transitions but produces finite values for $\Delta\tau=0,\ \pm 2$ transitions. The IBA parameters for the best IBA fit for ^{102}Pd are $\epsilon=0.76$ MeV, $a_0=0.18$ MeV, and $a_3=0.05$ MeV and, with $\eta=0.21$, they correspond to a structure very close to the critical point.

The corresponding total energy obtained using the intrinsic state formalism [5] is presented in Fig. 7. It is, indeed, close to a flat-bottomed shape, resembling the square well potential embodied in the E(5) symmetry, and close to the potential corresponding to the critical point for an IBA calculation for $N_B=5$ (also shown in Fig. 7).

Figure 8 compares the experimental low-lying level scheme and $B(E2)$ transition strengths (left) of ^{102}Pd with the E(5) symmetry (right) and with the best IBA fit (middle). Note that the E(5) predictions are parameter-free, except for scale. For the data in Fig. 8 we keep the conventional notation $0_2^+, 0_3^+$ and for the theoretical spectra we use the same

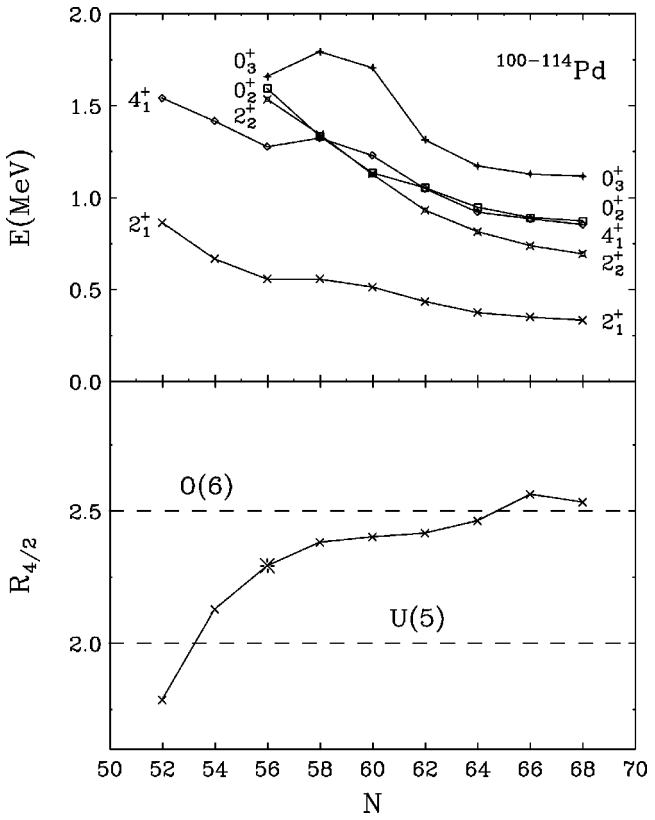

FIG. 5. The evolution of structure along the Pd isotopic chain. Top: Energies of the low-lying states. Bottom: $R_{4/2} \equiv E(4_1^+)/E(2_1^+)$. Note that ^{102}Pd, marked with a different symbol, is about halfway between the U(5) and O(6) limits.

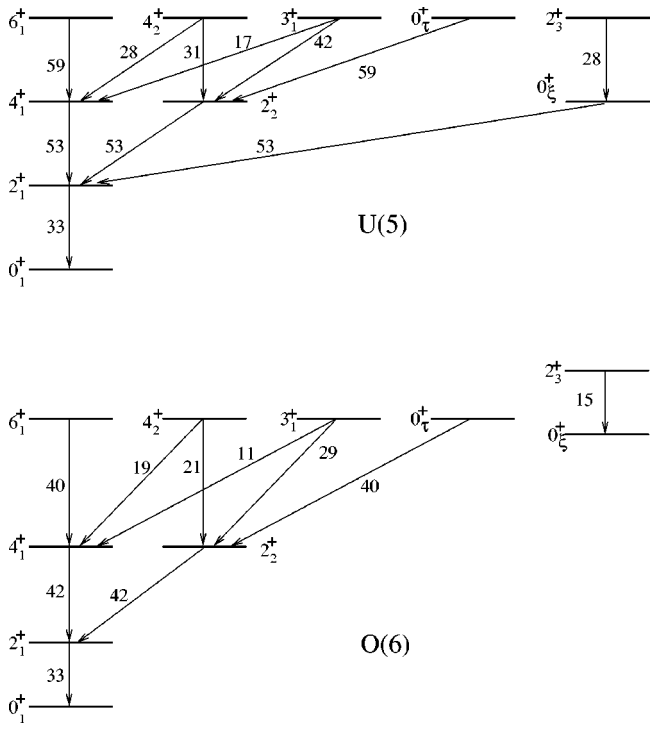

FIG. 6. Low-lying spectra of U(5) and O(6) for $N_B=5$. The state 0_τ^+ corresponds to the member of the three-phonon multiplet and the state labeled 0_ξ^+ corresponds to the $\sigma=N_B-2=\sigma_{max}-2$ O(6) state (see text). The energy of the 0_ξ^+ state in O(6) depends on an additional parameter and was chosen here, for an easy discussion, slightly lower than the 0_τ^+ state. The labels on the arrows denote $B(E2)$ values, normalized to $B(E2;2_1^+\rightarrow 0_1^+)=33$ W.u. (value corresponding to ^{102}Pd).

notation as in Fig. 6: the 0_τ^+ state is a member of the three-phonon multiplet and the 0_ξ^+ state is defined as the base state of the $\xi=2$ family of states in the E(5) description. The $0_\tau^+\rightarrow 2_1^+$ transition from the three-phonon 0^+ state is forbidden in U(5), O(6), and all along the transition leg since O(5) symmetry is preserved. Experimentally, in ^{102}Pd, the decay pattern of the 0_2^+ state is very similar to that of the theoretical 0_τ^+ state, and the state corresponding to 0_ξ^+ is the 0_3^+ level whose deexcitation to the 2_1^+ level is moderately collective (13 W.u.) with $B(E2{:}0_3^+\rightarrow 2_1^+)/B(E2{:}2_1^+\rightarrow 0_1^+)=0.39$, intermediate between U(5) and O(6).

The E(5) symmetry seems to reproduce the level energies of ^{102}Pd rather well, except for the energy of the 0_2^+ state, which is very different from the 0_τ^+ state. We will return to this below. First we consider the other levels and transitions. The data are reproduced, with a few exceptions [the experimental $B(E2;2_2^+\rightarrow 2_1^+)$ and $B(E2;4_2^+\rightarrow 4_1^+)$ values are less collective than predicted], by the E(5) symmetry. In Table II we compare the experimental values for key observables (except the properties of the 0_2^+ state) with the E(5) predictions and the numerical IBA calculations. The table shows that the experimental values of these observables are, indeed, between the U(5) and O(6) limits (also given in Table II). The other observables are also between these limits, as can be seen by comparing the data presented in Fig. 8 with the U(5) and O(6) predictions in Fig. 6.

The comparison of the data with the best-fit IBA results contained in Fig. 8 and Table II suggests that ^{102}Pd is indeed very close to the critical point of the transition between U(5) and O(6). The $R_{4/2}$ value is in good agreement with the data

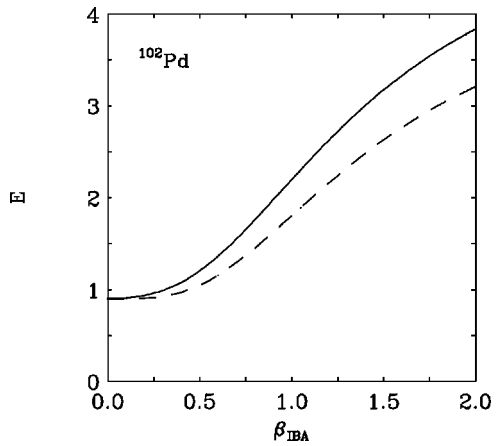

FIG. 7. Total energy obtained using the intrinsic state formalism as a function of the quadrupole deformation β_{IBA}. Continuous line: IBA parameters corresponding to ^{102}Pd ($N_B=5$, $\epsilon=0.76$ MeV, $a_0=0.18$ MeV, and $a_3=-0.05$ MeV); dashed line: IBA parameters corresponding to the critical point of the U(5)-O(6) transition.

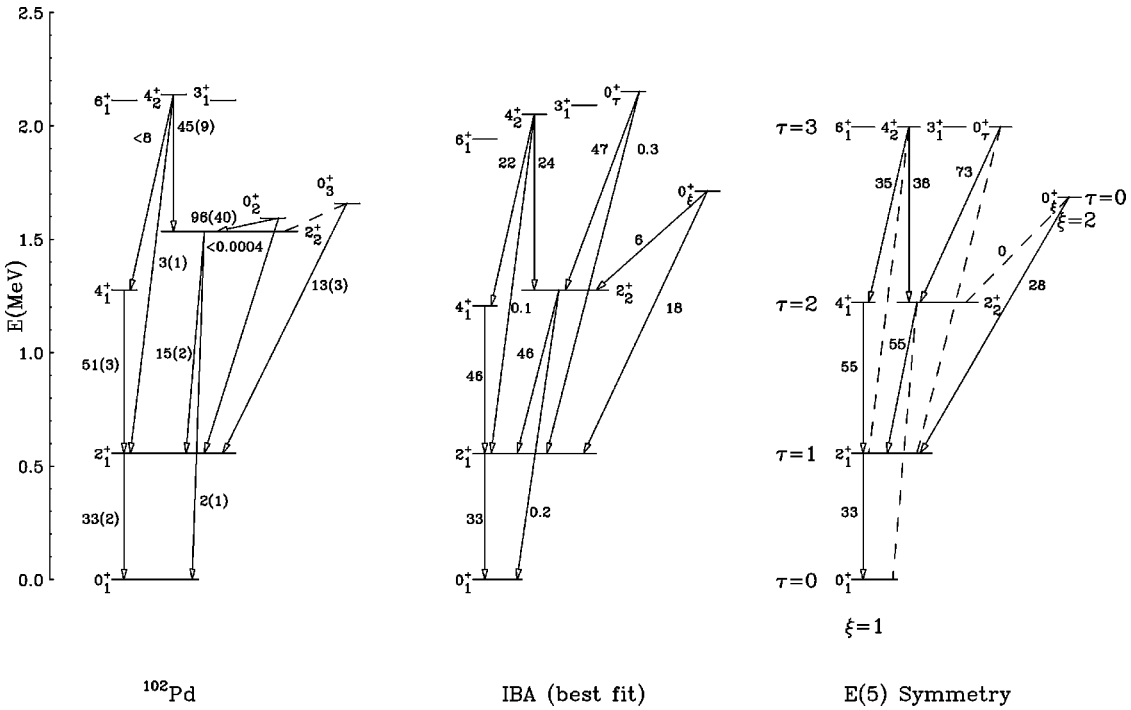

FIG. 8. Level scheme of ^{102}Pd (left) compared with the E(5) symmetry (right) and with IBA best-fit calculation (middle). The labels on the arrows denote the respective $B(E2)$ values in W.u. The experimental values are from Refs. [20,23] with the new γ-ray intensities reported in this work. Dashed lines denote unobserved transitions (expt.) or transitions with $B(E2)=0$ (theor.). The IBA parameters ($N_B=5$, $\epsilon=0.76$ MeV, $a_0=0.18$ MeV, and $a_3=0.05$ MeV) correspond to the control parameter $\eta=0.21$, which is slightly smaller than $\eta_{crit}=0.25$ in the transition between the anharmonic U(5) and O(6) limits. The $B(E2)$ values are obtained with the $T(E2)$ operator of Eq. (2) ($\chi=-\sqrt{7}/2$) and are given in W.u. [normalized to the experimental value $B(E2:2_1^+\rightarrow 0_1^+)=33$ W.u.].

and $E(0_\xi^+)/E(2_1^+)$ agrees almost exactly with the empirical energy ratio for the 0_3^+ state. In the E(5) symmetry the quadrupole transition strength was originally [6] calculated using a quadrupole operator, which depended linearly on the quadrupole deformation β [6]. A second-order term was introduced in the E(5) symmetry by Arias [25] and Frank *et al* [26] and the calculations with this operator are presented in Table II. Also included in Table II are predictions for E(5) for finite particle number [27]. All the E(5) predictions are in good agreement with the data; in particular, the calculations

TABLE II. Comparison of key observables in ^{102}Pd [20,23] with predictions of several models: IBA predictions for dynamical symmetries U(5) and O(6), for the critical point, and the best fit; E(5) predictions with a linear $T(E2)$ operator in the quadrupole deformation [6], including quadradic term in the $T(E2)$ operator [25], and E(5) for a finite well [27].

	Expt.	IBA				E(5)		
	^{102}Pd	U(5)	O(6)	Crit. pt.	Best fit	Ref. [6]	Ref. [25]	Ref. [27]
$R_{4/2}$	2.29	2.00	2.50	2.22	2.18	2.20	2.20	2.19
$\frac{E(0_\xi^+)}{E(2_1^+)}$ [a]	2.98[b]	2.00	c	3.54	3.10	3.03	3.03	2.99
$\frac{B(E2:4_1^+\rightarrow 2_1^+)}{B(E2:2_1^+\rightarrow 0_1^+)}$	1.56(13)	1.60	1.27	1.36	1.39	1.68	1.56	1.68
$\frac{B(E2:0_\xi^+\rightarrow 2_1^+)}{B(E2:2_1^+\rightarrow 0_1^+)}$ [a]	0.39(9)[b]	1.60	0	0.41	0.55	0.86	0.49	0.91

[a] 0_ξ^+ is defined as the base state of the $\xi=2$ family of states in the E(5) description or the base state of the $\sigma=N_B-2$ representation in O(6), and as a two-phonon state in U(5). In the IBA calculations for the critical point and for the best-fit calculations it is the first excited, or 0_2^+, level.
[b] Experimental 0_3^+ state corresponds to the theoretical 0_ξ^+ state in E(5).
[c] Undefined.

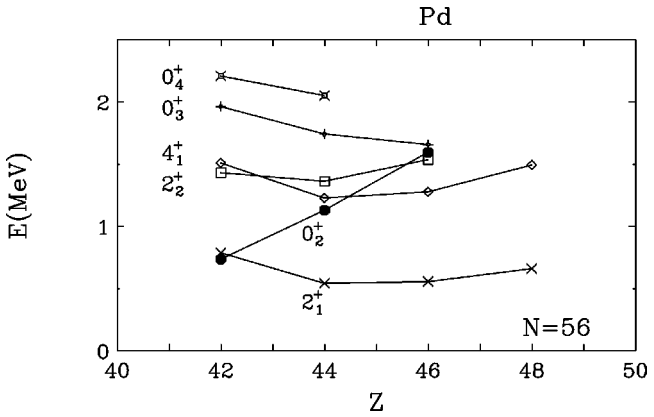

FIG. 9. Evolution of the energy of low-lying states along the $N=56$ isotonic chain.

of Ref. [25] nicely reproduce even the $B(E2)$ ratio for the 0_3^+ state.

Only the 0_2^+ state is difficult to accommodate in any of these pictures. Although its strong $B(E2)$ value for the transition to the 2_2^+ state agrees with the E(5) prediction for a member of the three-phonon multiplet and the corresponding E(5) 0_τ^+ state, the excitation energy disagrees strongly with E(5) (and with the IBA calculations). The $E0$ strength also disagrees with the E(5) symmetry: experimentally there is an $E0{:}0_2^+ \rightarrow 0_1^+$ transition reported [23], while in the E(5) symmetry the $E0{:}0_\tau^+ \rightarrow 0_1^+$ strength should be zero. These disagreements, especially the fact that its observed energy is much lower than predicted, suggest that the 0_2^+ state might represent a different degree of freedom outside the IBA space [i.e., it is not the E(5) 0_τ^+ state]. One possibility is that it could be an intruder state.

The lack of nucleon transfer data or knowledge of band structure built on the excited 0^+ states makes it difficult to definitively assert the intruder or nonintruder character of these states. However, indirect information on their structure can be obtained by studying their behavior along isotopic and isotonic chains. The evolution of the excited 0^+ state energies along the isotopic $Z=46$ chain, presented in Fig. 5 (top), does not show any irregular behavior that would suggest a deviation from a multiphonon picture.

However, the evolution of the 0_2^+ states as a function of proton number shows a very different behavior from other low-lying states. Figure 9 shows the data on low-lying level energies in the $N=56$ *isotonic* chain. The energy of the 0_2^+ state decreases toward $Z=40$, which is halfway between $Z=28$ and 50, and suggests that the 0_2^+ states in these isotones behave as intruder states. In fact, the 0_2^+ state was considered to be outside the IBA single shell space in previous analyses [14,15]. Higher excited 0^+ states are known only in the Mo and Ru nuclei with $N=56$. In the $^{98}_{42}$Mo$_{56}$ isotone the decay properties of the 0_3^+ state are unknown but in $^{100}_{44}$Ru$_{56}$ the branching ratio from the 0_3^+ state, $B(E2{:}0_3^+ \rightarrow 2_2^+)/B(E2{:}0_3^+ \rightarrow 2_1^+)=8$, is in agreement with the E(5) 0_τ^+ properties.

Based on these arguments, the 0_2^+ state in ^{102}Pd could be considered as an intruder state and the role of the 0_τ^+ state from an E(5) description could be played by a higher excited, as yet unknown, 0^+ state. Such a higher energy would be more consistent with an E(5) description of ^{102}Pd. In fact, in ^{104,106}Pd, a 0_4^+ state was identified very close in energy to the 6_1^+ state and in ^{106}Pd it preferentially decays to the 2_2^+ level, as expected for the 0_τ^+ level.

In assessing the intruder character of the 0_2^+ level in Pd isotopes, there is one caution that should be stressed. For the heavier Pd isotopes (up to $A=110$) strong $B(E2{:}2_3^+ \rightarrow 0_2^+)$ values ($\sim$100 W.u.) [28] have been used to suggest a *deformed* intruder configuration for the 0_2^+ levels [29]. The strong $0_2^+ \rightarrow 2_1^+$ transitions ($\sim$40 W.u.) in $^{106-110}$Pd suggest a different structure than that for the 0_2^+ level in ^{102}Pd, where the $B(E2{:}0_2^+ \rightarrow 2_1^+)$ value nearly vanishes. Therefore, the assignment of intruder structure to the 0_2^+ state in ^{102}Pd must not be taken to imply that the structure of the intruder is unchanged across the Pd isotopes.

IV. CONCLUSION

Levels in ^{102}Pd were populated in ϵ/β^+ decay and their properties were studied through γ-ray spectroscopy. Candidates for the 3^+ member of the three-phonon multiplet and for the 4^+ member of the four-phonon multiplet were established. The comparison with the predictions of the E(5) symmetry shows very good agreement, including the 0_3^+ state, which can be considered as the 0_ξ^+ state of E(5). The properties of the 0_2^+ state in ^{102}Pd and the evolution of this state along the $N=56$ isotonic chain suggest intruder character. Pending further experimental information on 0_i^+ $(i>3)$ states, ^{102}Pd is a very good candidate for the E(5) symmetry.

ACKNOWLEDGMENTS

This work was supported by the U.S. DOE under Grant Nos. DE-FG02-91ER-40609 and DE-FG02-88ER-40417 and by the DFG, Grant No. Pi393/1-1/1-2.

[1] G. Sharff-Goldhaber and J. Weneser, Phys. Rev. **98**, 212 (1955).
[2] A. Bohr, Mat. Fys. Medd. K. Dan. Vidensk. Selsk. **26**(14) (1952).
[3] L. Wilets and M. Jean, Phys. Rev. **102**, 788 (1956).
[4] F. Iachello and A. Arima, *The Interacting Boson Model* (Cambridge University Press, Cambridge, England, 1987).
[5] A.E.L. Dieperink, O. Scholten, and F. Iachello, Phys. Rev. Lett. **44**, 1747 (1980).
[6] F. Iachello, Phys. Rev. Lett. **85**, 3580 (2000).
[7] F. Iachello, Phys. Rev. Lett. **87**, 052502 (2001).
[8] R.F. Casten and N.V. Zamfir, Phys. Rev. Lett. **85**, 3584 (2000).
[9] R.F. Casten and N.V. Zamfir, Phys. Rev. Lett. **87**, 052503 (2001).

[10] R. Krücken *et al.* (unpublished).
[11] J. Stachel, P. Van Isacker, and K. Heyde, Phys. Rev. C **25**, 650 (1982).
[12] D. Bucurescu, G. Cata, D. Cutoiu, G. Constantinescu, M. Ivascu, and N.V. Zamfir, Z. Phys. A **324**, 387 (1986).
[13] P. Van Isacker and G. Puddu, Nucl. Phys. **A348**, 125 (1980).
[14] Ka-Hae Kim, A. Gelberg, T. Mizusaki, T. Otsuka, and P. von Brentano, Nucl. Phys. **A604**, 163 (1996).
[15] A. Giannatiempo, A. Nanini, and P. Sona, Phys. Rev. C **58**, 3316 (1998).
[16] Feng Pan and J.P. Draayer, Nucl. Phys. **A636**, 156 (1998).
[17] O.K. Vorov and V.G. Zelevinsky, Nucl. Phys. **A439**, 207 (1985).
[18] N.V. Zamfir and R.F. Casten, J. Res. Natl. Inst. Stand. Technol. **105**, 147 (2000).
[19] A. Gavron, Phys. Rev. C **21**, 230 (1980).
[20] D. de Frenne and E. Jacobs, Nucl. Data Sheets **83**, 535 (1998).
[21] K. Cornelis, G. Lhersonneau, M. Huyse, D. Vandeplassche, and J. Verplancke, Z. Phys. A **292**, 403 (1979).
[22] J. Van Klinken, S.J. Feenstra, K. Wisshank, and H. Faust, Nucl. Instrum. Methods **130**, 427 (1975).
[23] M. Luontama, R. Julin, J. Kantele, A. Passoja, W. Trzaska, A. Bäcklin, N.G. Jonsson, and L. Westerberg, Z. Phys. A **324**, 317 (1986).
[24] K. Farzin, H. Hardenberg, H. Möllmann, K. Uebelgünn, and H.v. Buttlar, Z. Phys. A **326**, 401 (1987).
[25] J.M. Arias, Phys. Rev. C **63**, 034308 (2001).
[26] A. Frank, C.E. Alonso, and J.M. Arias, Phys. Rev. C **65**, 014301 (2002).
[27] M. A. Caprio, Phys. Rev. C **65**, 031304(R) (2002).
[28] L.E. Svensson, C. Fahlander, L. Hasselgren, A. Bäcklin, L. Westerberg, D. Cline, T. Czosnyka, C.Y. Wu, R.M. Diamond, and H. Kluge, Nucl. Phys. **A584**, 547 (1995).
[29] J.L. Wood, K. Heyde, W. Nazarewicz, M. Huyse, and P. van Duppen, Phys. Rep. **215**, 101 (1992).